275 *Egypt. J. Chem.* **Vol. 67,** No. 6 pp. 225 - 232 (2024)

Egyptian Journal of Chemistry

http://ejchem.journals.ekb.eg/

Multi-step differential transform method for both Hall currents and mixed convection effects on MHD flow of non-Newtonian fluid with Al_2O_3 nanoparticles

M. Y. Abou-zeid[1] and M. G. Ibrahim[2*]

[1] *Department of Mathematics, Faculty of Education, Ain Shams University, Heliopolis, Cairo, Egypt.*

[2]*Department of Basic and Applied Science, Faculty of Engineering, IAEMS, Cairo, Egypt*.

Abstract

Mixed convection MHD peristaltic flow of Prandtl nanofluid is constructed. A flow is affected by activation energy, hall current variable velocity slip conditions, and thermal radiation through a non-uniform channel. Governing equation describes the fluid model in a system of PDEs, and then non-dimensional quantities, and the assumption of long wavelength and low Reynolds number are used to obtain a system of ODEs. The leading system's results are constructed by an analytical method called a multi-stage differential transform method (Ms-DTM). All obtained graphical results are proposed in terms of y versus different fluid distributions. An analytical solution is shown through a table that offered a numerical interest result. Outcomes show that the growth in variable velocity slip causes a rise in fluid velocity distribution. Applications like drug carriers can get more opportunities through studies of the present system.

Keywords: Double-diffusivity; non-constant velocity slip; Thermal convection; Prandtl nanofluid; Ms-DTM; *Mathematica 13.0.1*.

1 Introduction

Non-Newtonian have vital and different uses in most life fields when shaken the Ketchupis are considered as a non-Newtonian fluid example, polymers, paint, blood, shampoos, etc…. A non-constant fluid thermal conductivity effect on a non-Newtonian nanofluid is proposed by Mahmood et al [1] and shows that a non-Newtonian fluid combined with nano techniques has a vital role in most of the obtainable energy processes. Ibrahim [2], [3], and [4] use a non-Newtonian fluid mechanism in many drug carriers system. In the field of petroleum processes, Hasona et al [5] studied the non-constant viscosity effect on a non-Newtonian nanofluid with a magnetic field. Generally, a non-Newtonian fluid is a fluid that does not follow Newton's law of viscosity, in non-Newtonian fluids, the viscosity can be varied when pressurized to either a more liquid or a more solid one. A non-Newtonian fluid has had countless vital and various applications in the last decades by modelers and investigators, for more applications see Refs .[20-6] .

A "nanofluid" is a heat transfer fluid that contains "nanoparticles" (suspended nanoparticles) with sizes ranging from 1 to 100 nm dispersed throughout the base fluid. In the present study, we assume the two-phase model, i.e. both Brownian and thermophoresis effects will appear in the governing equations system. Morevere, rhe nanoparticles Al2 O3 is used with base fluid to shape nanofluid. Nanofluids can be studied theoretically or experimentally in order to control the process of heat transfer. There are two ways to simulate nanofluids, namely, single- and two-phase. Nanofluids is treated as the common pure fluid in single-phase model, and there aren't any slip velocities between the nanoparticles and fluid molecules. In two-phase model, the researchers consider that there are slip velocities between the nanoparticles and fluid molecules. So, there would be a variable concentration of nanoparticles in a mixture. Also, the velocity between the fluid and particles may not be vanished due to many factors such as friction between the fluid and solid particles, Brownian forces, gravity, Brownian diffusion, thermophoresis properties and dispersion. While in single-phase model, the nanoparticles can be easily fluidized, and therefore, it can be assumed that the motion slip between the phases would be considered negligible. In the present study, we assume the two-phase model, i.e. both Brownian and thermophoresis effects will appear in the governing equations system. Morevere, table (1) analyzed the thermal properties of Al2 O3-water Nanofluid.

Physical properties	Fluidphase (water)	Al2 O3
C_p (J/kg K)	4179	4181
ρ (kg/m^3)	997.1	3600
k (W/m K)	0.613	0.617

Table 1. Thermophysical properties of basefluid (water) and Al2 O3 nanoparticles.

Nowadays, energy has a vital role in all recent applications of engineering, chemical, and physical processes, so, it has attracted the attention of modelers, researchers, and engineers. Generally, activation energy is the energy that is necessary to be provided to a chemical or nuclear system of latent reactants to cause a nuclear, and chemical reaction or countless other physical phenomena. Further, the term was coined by the Swedish chemist Svante Arrhenius in 1889 **[21]**. Shafique et al **[22]** addressed the

*Corresponding author e-mail: drmohamedibrahim2023@gmail.com (M. G. Ibrahim).
Receive Date: 18 October 2023, Revise Date: 15 November 2023, Accept Date: 29 November 2023
DOI: 10.21608/EJCHEM.2023.243470.8748

rotating frame in boundary flow in presence of activation energy; they found that the parameter of activated energy grows in the temperature of the fluid. Gowda et al **[23]** discussed the velocity profile for the boundary layer flow with the activation energy effect. In nearly times, applications of activation energy appeared more and more in different fields like nuclear reactions in engineering **[24]**, and various physical phenomena in physics **[25, 26],** and many applications of such fluids can be found in Refs. **[27-30]**.

The slip velocity is defined as the variance in velocities among liquids in the flow of two-phase mixtures over a pipe because of the slip between the two phases. Further, in hearts valves slip velocity comes at the highest of its authentication **[31]**. Nisar et al **[32]** deliberated the MHD peristaltic flow of Eyring Powell nanofluid in presence of activation energy influences. They found that the high standards of slip parameters increase the velocity profile. Akbar and Nadeem **[33]** suggest a new model for Jeffrey's fluid under slip effects. They found that the increases in pressure rise advances rise the slip factor. In Refs. **[1-28]** slip velocity is mentioned in some of the like **[1, 6, 10, 26-28]** as it's paramount in artificial heart valves. Supplementary, the other investigation doesn't acquaint about it. In the present manuscript, the variable slip velocity is considered to declare its significant part in the valves of the heart **[34-35]**.

The novelty/uniqueness of the proposed article is to present a theoretical recommendation in the relations of velocity slip conditions and thermal radiation effects on magneto-nano Prandtl fluid in a tapered channel. The fluid profile behavior is achieved as graphs using a Ms-DTM. The This physical modeling is essential for some physiological flows, such as the flow of stomach juice during the insertion of an endoscope.The formulation of the problem is introduced through the following section; the solution method of the present model is presented in section three; analysis of sketches/results is offered in section four; section five introduces the main points/conclusions of the present work.

2 Formulation problem

In the Cartesian coordinate (x, y), the velocity slip and hall current effects on the peristaltic flow of Prandtl nanofluid in a tapered symmetric channel are considered. Thermal radiation has affected the flow and the magnetic field (B_0) influence in the $y - axis$, and perpendicular to $x - axis$ see **Figure 1. [16].**

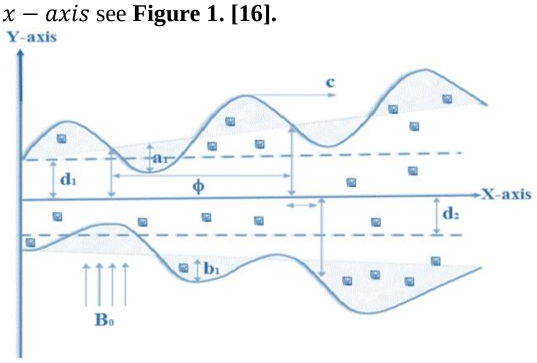

Fig. 1: Physical model graph

$$y = \hat{h}(\hat{x}, \hat{t}) = \pm a_1(\hat{x}) \pm b\, Sin\, \frac{2\pi}{\lambda}(\hat{x} - c\hat{t}) \quad (1)$$

$$a_1(\hat{x}) = a_0 + \overline{m}\hat{x} \quad (2)$$

Where the variable width $a_1(\hat{x})$ of the channel, the amplitude (b) wave, the velocity of (c) propagating wave, the value of half-width (a_0)at the inlet, the time $(\hat{t})$, the axial $(\hat{x})$ space, the wavelength (λ), the non-uniform (m) parameter, respectively. The axial velocity is defined as $\hat{V} = [\hat{U}(\hat{X}, \hat{Y}, \hat{t}), \hat{V}(\hat{X}, \hat{Y}, \hat{t}), 0]$.

Prandtl fluid extra stress tensor is obtainable as follows [**11 − 13**]:

$$\boldsymbol{S} = \left[\frac{A\, sin^{-1}\left[\frac{1}{B}\left(\frac{\partial u}{\partial y}\right)^2 + \left(\frac{\partial v}{\partial x}\right)^2\right]^{\frac{1}{2}}}{\left[\left(\frac{\partial u}{\partial y}\right)^2 + \left(\frac{\partial v}{\partial x}\right)^2\right]^{\frac{1}{2}}}\right]\frac{\partial u}{\partial y}, \quad (3)$$

Where the material constants of the tensor are A and B.

The thermal radiation is labeled as:

$$q_r = -\frac{-4\sigma^*}{3\,k^*}\frac{\partial T^4}{\partial y}, \quad (4)$$

The governing equation of incompressible fluid is constructed in the laboratory frame $(\hat{X}, \hat{Y})$ as follows [36-43]:

$$\frac{\partial \hat{U}}{\partial \hat{X}} + \frac{\partial \hat{V}}{\partial \hat{Y}} = 0, \quad (5)$$

$$\rho_f\left(\frac{\partial}{\partial \hat{t}} + \hat{U}\frac{\partial}{\partial \hat{X}} + \hat{V}\frac{\partial}{\partial \hat{Y}}\right)\hat{U} = -\frac{\partial \hat{P}}{\partial \hat{X}} + \frac{\partial}{\partial \hat{X}}\boldsymbol{S}_{\hat{X}\hat{X}} + \frac{\partial}{\partial \hat{Y}}\boldsymbol{S}_{\hat{X}\hat{Y}} - \frac{\sigma B_0^2}{1+m_1^2}\hat{U} + g\{(1 - \hat{\Upsilon}_0)\rho_f\{\beta_{\hat{T}}(\hat{T} - \hat{T}_0) + \beta_{\hat{C}}(\hat{C} - \hat{C}_0)\} - (\rho_p - \rho_{f0})(\hat{\Upsilon} - \hat{\Upsilon}_0)\}, \quad (6)$$

$$\rho_f\left(\frac{\partial}{\partial \hat{t}} + \hat{U}\frac{\partial}{\partial \hat{X}} + \hat{V}\frac{\partial}{\partial \hat{Y}}\right)\hat{V} = -\frac{\partial \hat{P}}{\partial \hat{Y}} + \frac{\partial}{\partial \hat{X}}\boldsymbol{S}_{\hat{Y}\hat{X}} + \frac{\partial}{\partial \hat{Y}}\boldsymbol{S}_{\hat{Y}\hat{Y}} - \sigma B_0^2\hat{V}, \quad (7)$$

$$(\rho c)_f\left(\frac{\partial}{\partial \hat{t}} + \hat{U}\frac{\partial}{\partial \hat{X}} + \hat{V}\frac{\partial}{\partial \hat{Y}}\right)\hat{T} = -\frac{\partial \hat{q}_r}{\partial y} + k\left(\frac{\partial^2 \hat{T}}{\partial \hat{X}^2} + \frac{\partial^2 \hat{T}}{\partial \hat{Y}^2}\right) + (\rho c)_p\left\{D_B\left(\frac{\partial \hat{\Upsilon}}{\partial \hat{X}}\frac{\partial \hat{T}}{\partial \hat{X}} + \frac{\partial \hat{\Upsilon}}{\partial \hat{X}}\frac{\partial \hat{T}}{\partial \hat{X}}\right) + \frac{D_{\hat{T}}}{\hat{T}_0}\left[\left(\frac{\partial \hat{T}}{\partial \hat{X}}\right)^2 + \left(\frac{\partial \hat{T}}{\partial \hat{Y}}\right)^2\right]\right\} + D_{\hat{T}\hat{C}}\left(\frac{\partial^2 \hat{C}}{\partial \hat{X}^2} + \frac{\partial^2 \hat{C}}{\partial \hat{Y}^2}\right) + \frac{\sigma B_0^2}{1+m_1^2}B_0^2(U + V^2), \quad (8)$$

$$\left(\frac{\partial}{\partial \hat{t}} + \hat{U}\frac{\partial}{\partial \hat{X}} + \hat{V}\frac{\partial}{\partial \hat{Y}}\right)\hat{C} = D_s\left(\frac{\partial^2 \hat{C}}{\partial \hat{X}^2} + \frac{\partial^2 \hat{C}}{\partial \hat{Y}^2}\right) + D_{\hat{C}\hat{T}}\left(\frac{\partial^2 \hat{T}}{\partial \hat{X}^2} + \frac{\partial^2 \hat{T}}{\partial \hat{Y}^2}\right), \quad (9)$$

$$\left(\frac{\partial}{\partial \hat{t}} + \hat{U}\frac{\partial}{\partial \hat{X}} + \hat{V}\frac{\partial}{\partial \hat{Y}}\right)\hat{\Upsilon} = D_B\left(\frac{\partial^2 \hat{\Upsilon}}{\partial \hat{X}^2} + \frac{\partial^2 \hat{\Upsilon}}{\partial \hat{Y}^2}\right) + \frac{D_{\hat{T}}}{\hat{T}_0}\left(\frac{\partial^2 \hat{T}}{\partial \hat{X}^2} + \frac{\partial^2 \hat{T}}{\partial \hat{Y}^2}\right), \quad (10)$$

Where the stress $(\hat{\boldsymbol{S}})$ tensor of Prandtl fluid, the particles (ρ_p) density, the base (ρ_f) fluid density, the fluid (ρ_{f0}) density at T_0, the body (f) force, the fluid $(\beta_{\hat{C}})$ volumetric solutal $(\beta_{\hat{T}})$ expansion, the flow $(\hat{T})$ temperature, concentration $(\hat{C})$ and nanoparticle volume$(\hat{\Upsilon})$ fraction respectively, the Brownian (D_B) diffusion, the acceleration (g) due to gravity, the thermophoresis $(D_{\hat{T}},)$ diffusion, the fluid $((\rho c)_f)$ heat capacity, the sort $(D_{\hat{C}\hat{T}})$ diffusively, the material time $(\frac{d}{dt})$ derivative the solutal (D_s) diffusively, the nanoparticle $((\rho c)_p)$ heat capacity, DuFour $(D_{\hat{T}\hat{C}})$ diffusively,

fixed frame (X, Y) defines the unsteady flow, while in a wave frame motion (x, y) is used. The wave and fixed frame relations are considered as the following:

$$p(x, y) = \hat{P}(\hat{X}, \hat{Y}, t), x = \hat{X} - ct, y = \hat{Y}, u = \hat{U} - c, v = \hat{V}, \quad (11)$$

Levy the dimensionless parameters as follows:

$\hat{x} = \frac{x}{\lambda}, \hat{y} = \frac{y}{b_0}, \hat{t} = \frac{ct}{\lambda}, \hat{v} = \frac{v}{c}, u = \frac{\partial \psi}{\partial y}, v = -\delta \frac{\partial \psi}{\partial x}, \delta = \frac{b_0}{\lambda}$ is the wave number, $\hat{p} = P\frac{b_0^2}{\mu c \lambda}$ is the pressure, $Re = \frac{c\rho_f b_0}{\mu}$ is the Reynolds number, $\Omega = \frac{\hat{\Upsilon}-\hat{\Upsilon}_0}{\hat{\Upsilon}_1-\hat{\Upsilon}_0}$ is the nanoparticle fraction , $\theta = \frac{\hat{T}-\hat{T}_0}{\hat{T}_1-\hat{T}_0}$ is the temperature, $\varphi = \frac{\hat{C}-\hat{C}_0}{\hat{C}_1-\hat{C}_0}$ is the concentration, $P_r = \frac{(\rho c)_f \nu}{\kappa_0}$ is the Prandtl number , $Le = \frac{\nu}{D_s}$ is the Lewis number, $S_c = \frac{(\hat{T}_1-\hat{T}_0)D_{\hat{C}\hat{T}}}{D_s(\hat{C}_1-\hat{C}_0)}$ is the Dufour parameters, $S_r = \frac{(\hat{C}_1-\hat{C}_0)D_{\hat{T}\hat{C}}}{(\hat{T}_1-\hat{T}_0)\varsigma}$ is the Soret parameter, $M = \sqrt{\frac{\sigma}{\mu}}b_0 B_0$ is the Hartmann number, $G_r = \frac{g b_0^2(1-\hat{\Upsilon})\rho_f \beta_{\hat{T}}(\hat{T}_1-\hat{T}_0)}{\mu_0 c}$ is the thermal Grashof numbers, $G_c = \frac{g b_0^2(1-\hat{\Upsilon})\rho_f \beta_{\hat{C}}(\hat{C}_1-\hat{C}_0)}{\mu_0 c}$ is the nanoparticle Grashof numbers, $G_F = \frac{g b_0^2(\rho_p-\rho_f)b_0^2(\hat{\Upsilon}_1-\hat{\Upsilon}_0)}{\mu_0 c}$ is the solutal Grashof numbers, $Ln = \frac{\nu}{D_B}$ is the nanofluid Lewis number, $N_t = \frac{(\rho c)_p D_T(\hat{T}_1-\hat{T}_0)}{\hat{T}_0 \varsigma}$ is the thermophoresis parameters and $N_b = \frac{(\rho c)_p D_B(\hat{\Upsilon}_1-\hat{\Upsilon}_0)}{\varsigma}$ is the Brownian motion parameter, $R = \frac{4\sigma^*}{3k^*}\frac{T_0^3}{\varsigma c_f}$ is the parameter of thermal radiation, $B_r = E_c$ Eckret number $\times P_r$.

by using the above-mentioned non-dimensional parameters and dropping the pars, the system of equations (5-10) becomes.

$$-\frac{\partial p}{\partial x} + \frac{\partial}{\partial y}\left(\sigma \frac{\partial^2 \psi}{\partial y^2} + \frac{\beta_1}{6}\left(\frac{\partial^2 \psi}{\partial y^2}\right)^3\right) - \frac{M^2}{1+m_1^2}Cos(\beta)^2\left(\frac{\partial \psi}{\partial y} + 1\right) + G_r\,\theta + G_c\,\varphi - G_r\,\Omega = 0, \quad (12)$$

$$\frac{\partial p}{\partial y} = 0, \quad (13)$$

$$(1+R_d)\frac{\partial^2 \theta}{\partial y^2} + B_r\left(\sigma \frac{\partial^2 \psi}{\partial y^2} + \beta_1\left(\frac{\partial^2 \psi}{\partial y^2}\right)^3\right)\frac{\partial^2 \psi}{\partial y^2} + P_r N_t\left(\frac{\partial \theta}{\partial y}\right)^2 + P_r N_b \frac{\partial \theta}{\partial y}\frac{\partial \varphi}{\partial y} - \frac{M^2}{1+m_1^2}\left(\frac{\partial \psi}{\partial y} + 1\right)^2 + S_r\frac{\partial^2 \Omega}{\partial y^2} = 0, \quad (14)$$

$$\frac{\partial^2 \varphi}{\partial y^2} + S_c\frac{\partial^2 \theta}{\partial y^2} - (\rho\,\theta + 1)\,\varphi\, e^{\frac{-E}{(\rho\,\theta+1)}} = 0, \quad (15)$$

$$\frac{\partial^2 \Omega}{\partial y^2} + \frac{N_t}{N_b}\frac{\partial^2 \theta}{\partial y^2} = 0. \quad (16)$$

Use Eqs. (13) and (14) then we have:

$$\frac{\partial^2}{\partial y^2}\left(\sigma \frac{\partial^2 \psi}{\partial y^2} + \frac{\beta_1}{6}\left(\frac{\partial^2 \psi}{\partial y^2}\right)^3\right) + G_r\frac{\partial \theta}{\partial y} + G_c\frac{\partial \varphi}{\partial y} - G_F\frac{\partial \Omega}{\partial y} - \frac{M^2}{1+m_1^2}Cos(\beta)^2\frac{\partial}{\partial y}\left[\left(\frac{\partial \psi}{\partial y} + 1\right)\right] = 0, \quad (17)$$

The extra stress ($\boldsymbol{S_{xy}}$) tensor is abstracted as the following using the non-dimensional parameter.

$$\boldsymbol{S_{xy}} = \sigma\frac{\partial^2 \psi}{\partial y^2} + \frac{\beta_1}{6}\left(\frac{\partial^2 \psi}{\partial y^2}\right)^3, \quad (18)$$

The extra tensor parameter is $\sigma = \frac{A}{\mu\, B}$, and $\beta_1 = \frac{\alpha_1 c^2}{B^2 b_0}$.

The variable velocity slip mechanism with thermal slip constraints is constructed as follows **[4]**:

$$U' - U'_w = \xi s_{xy}, \quad (19)$$

Where, the velocity $U'_w$of the wall, velocity (ξ) slips in a variable case. So, the appropriate boundary conditions are as:

$$\psi = 0, \frac{\partial^2 \psi}{\partial y^2} = 0, \theta = 0, \varphi = 0, \Omega = 0 \ at\ y = 0 \quad (20)$$

$$\psi = q, \frac{\partial \psi}{\partial y} + \xi\left(\sigma\,\frac{\partial^2 \psi}{\partial y^2} + \beta_1\left(\frac{\partial^2 \psi}{\partial y^2}\right)^3\right) = -1, \theta = 1, \varphi = 1, \Omega = 1\ \ at\ y = 1 + mx + \beta_2\,\mathrm{Sin}[2\pi x], \quad (21)$$

Eq. (20) implies that the fluid particles closest to the uniform wall of channel are at rest and both temperature, concentration and nanoparticles are vanish, while in Eq. (21) they are equal to unity on the wavy boundary and the stream lines occur when the liquid to wavy boundary flow is not applied evenly.

3 Method of solution

Firstly, the system of ordinary differential equations (14-17) is transformed using the theories of the differential transform method. Consequently, the initial values of boundary conditions are obtained, and then the interval of a solution is subdivided into sub-intervals. The solution of a system is obtained at each of the sub-intervals and the results are improved. Multi-stage differential transform method is used to overcome the divergence in the solutions. Many steps used in computer program algorithms use Wolfram Mathematica version 13.0.1.

Let:

$$y(t, f, f', \ldots, f^{(n)}) = 0. \quad (22)$$

Related to the following conditions

$$f^{(k)}(0) = d_k,\ k = 0, \ldots, n-1. \quad (23)$$

The finite series solution will take the form

$$f(t) = \sum_{k=0}^{N} F(k)(t - t_0)^{(k)},\ \forall t \in D. \quad (24)$$

The Ms-DTM solution of ODEs (14-17) is as follows:

$$\psi(y) = \sum_{n=0}^{N} \Psi[k] y^n \quad (25)$$

$$\theta(y) = \sum_{n=0}^{N} \Theta\,[k] y^n \quad (26)$$

$$\varphi(y) = \sum_{n=0}^{N} \Phi[k] y^n \quad (27)$$

$$\Omega(y) = \sum_{n=0}^{N} \Upsilon[k] y^n \quad (28)$$

Now, the skin friction (τ_w) coefficient, Nusselt number(Nu) coefficient, and Sherwood (Sh) number are defined as,

$$\tau_w = \left(\frac{\beta_1}{6}\left(\frac{\partial^2 \psi}{\partial y^2}\right)^3 + \sigma\frac{\partial^2 \psi}{\partial y^2}\right)\Big|_{y=h}, Nu = \frac{\partial \theta}{\partial y}\Big|_{y=h}, Sh = \frac{\partial \varphi}{\partial y}\Big|_{y=h}, \quad (29)$$

The achieved results will be debated in the next sections.

4. Results and discussion

This section proposes numerical and graphical results for a system of equations (14-17) using the analytical method called Ms-DTM. In a Table (2) numerical results for skin (τ_w) friction coefficient, Nusselt (Nu) number coefficient, and Sherwood (Sh) number versus a different values of Hall ($m1$) current and slip (ξ) parameter are presented. τ_w, and Nu are considered as an increasing function in hall current values, while Sh has a declining values at high values of $m1$. slip parameter values on (τ_w), (Nu) and (Sh) has a contradict effects than found in Hall ($m1$) current, which shows that there are an inverse correlation between Hall and slip parameters.

Table 2: Various values of (τ_w), (Nu) and (Sh) versus values of Hall current number, and slip parameter

$m1$	ξ	τ_w	Nu	Sh
0	0.1	1.2255800812887	0.0376272328467	0.02636226954287
0.1	-	1.2261770032773	0.0377776079230	0.02631917138882
0.5	-	1.237772872928	0.04069668843515	0.02548250778745
1	-	1.256597111988	0.0454310594172	0.02412537436136
5	-	1.286819401240	0.0530413321478	0.02194339476581
10	-	1.288739990545	0.0535260242035	0.02180440740648
1	0.0	1.4262326872003	0.0456844396408	0.02406357325725
-	0.1	1.3821890811212	0.0455872759931	0.02408831580619
-	0.3	1.3117762607421	0.04547939761894	0.02411471622028
-	0.5	1.2565971119883	0.04543105941723	0.024125374361365
-	0.7	1.2113238297585	0.04541231028090	0.024128328344952
-	0.9	1.1730354499454	0.04540964712007	0.024127175181709

Figures 2-13 are proposed to study the behavior of different values of intersetd parameters versus a districutions of fluid. Figs. 2 shows that the slip parameter has a dual role on the velocity profile. That's mean, a high values of ξ causes a velocity profile diminshing in the interval $y \in [0, 0.6984]$, while it growing in the interval $y \in [0.6992, 1.243]$. It's depicted from Figs. 3,and 4 that the vlocity distribtion growing in the left part of channel and diminishing in the right part of the channel with a growing values of G_F and m_1. Finally, more sight effects are shown in the case of high values in solutal Grashof number.

Temperature distribution is studied against hall parameter, slip parameter, and thermal radiation through sketches 5, 6, and 7. Results shows that the hall and slip parameters have a like behavior on the temperature profile, through Figs. 5, and 6. Physically, the particels get more effective energy at high values of hall and slip parameters, which gets the particle move more freely to support the drug delivery stystem. Fig. 7 displays that the thermal radiation diminshes the temperature profile. The numerical values of Activation energy E_a and thermophoresis parameters (N_t) are studied versus concentration profile. It's illustrated from Figs. 8, and 9 that the high values of Activation energy (E_a) and thermophoresis parameters (N_t) have an opposite behavior on concentration profile. Concentration distribution is considerd as an increasing function in E_a and decreasing function in N_t.

Nanoparticle fraction behavior are studied against various paremeters of interest throgh Figs. 10, 11, 12, and 13. It's portrayed from Figs. 10, and 11 that the growths in thermal radiation and Hartmann number causes a growth in the Nanoparticle fraction profile. Furthermore, insight behavior is visulaized in case of Hartmann number than found in the thermal radiation. As acontradiction, the beahvior of high values of reaction parameter and Hall current leads to a diminshing in the profile of Nanoparticle friction.

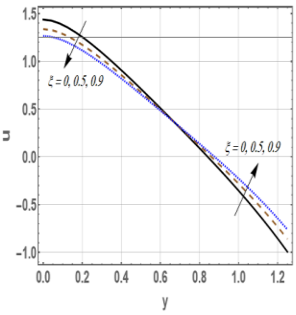

Fig. 2: Pofile of velocity $u(y)$ versus ξ.

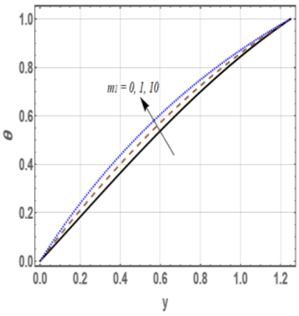

Fig. 5: Profile of Tempertaure $\theta(y)$ versus m_1.

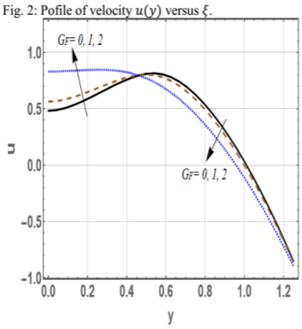

Fig. 3: Pofile of velocity $u(y)$ versus G_F.

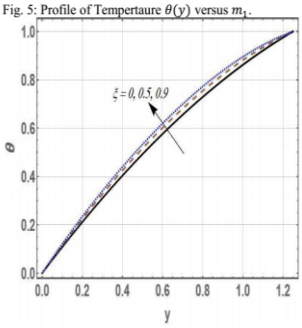

Fig. 6: Profile of Tempertaure $\theta(y)$ versus ξ.

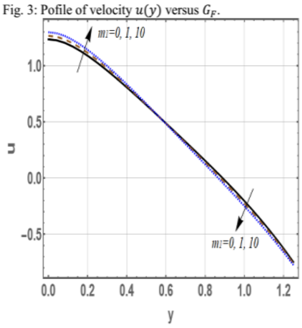

Fig. 4: Pofile of velocity $u(y)$ versus m_1.

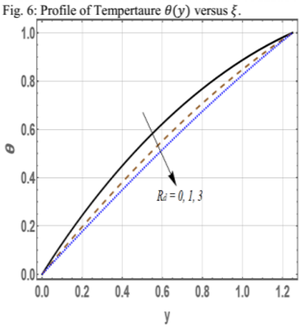

Fig. 7: Profile of Tempertaure $\theta(y)$ versus R_d.

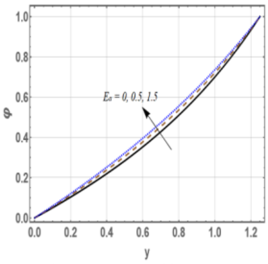

Fig. 8: Profile of Concentration $\varphi(y)$ versus E_a.

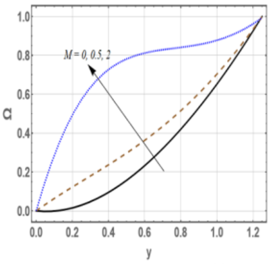

Fig. 11: Profile of Nanoparticle Friction $\Omega(y)$ versus M.

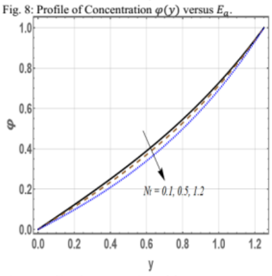

Fig. 9: Profile of Concentration $\varphi(y)$ versus N_t.

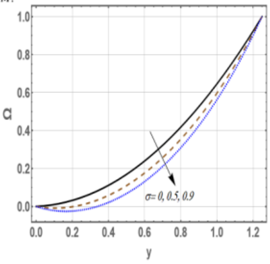

Fig. 12: Profile of Nanoparticle Friction $\Omega(y)$ versus ξ.

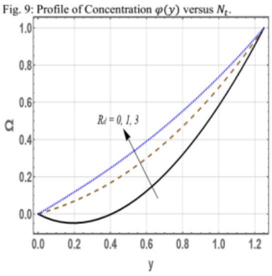

Fig. 10: Profile of Nanoparticle Friction $\Omega(y)$ versus R_d.

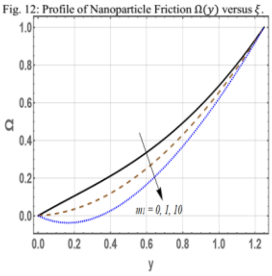

Fig. 13: Profile of Nanoparticle Friction $\Omega(y)$ versus m_1.

5 Conclusion

The outcomes of this paper is sheds light on the Hall current, slip velocity in variable case, and activation energy effects on the Prandtl nanofluid flow in an non-uniform channel. The analytical solutions are obtained use the multi-stage differential transform method. Graphical and numerical results are obtained with aid of Mathematica program version 13.0.1. The numerical results for various values of (τ_w), (Nu) and (Sh) versus values of Hall current number, and slip parameter are showed through Table 2. In addition, it is predicted that the current problem will lead to treat with some multifaceted difficulties in industry, engineering [44-66]. The main conclusions of proposed paper is as follows:

- Inverse correlation between Hall and slip parameters are obtained on (τ_w), (Nu) and (Sh).
- Hartman number and Hall Parameter have a like behavior on profile of Nanoparticle friction.
- Without lineraization or perturbation, accurate results are obtained using Ms-DTM.
- Varaible velocity slip parameter has an opposite performance on Nanoparticle friction.
- A dual role phenomena is observed on the fluid velocity distribution vesrsus different values of parameters like G_F, m_1, and ξ.

References

1- A. Mahmood, A. Aziz, W. Jamshed, and Sajid Hussain, Mathematical model for thermal solar collectors by using magnetohydrodynamic Maxwell nanofluid with slip conditions, thermal radiation and variable thermal conductivity, Results in Physics 7 (2017) 3425–3433.

2- M. G. Ibrahim, Computational calculations for temperature and concentration-dependent density effects on creeping motion of Carreau fluid: biological applications, Waves in Random and Complex Media, 32, 2022.

3- M. G. Ibrahim, Concentration-dependent electrical and thermal conductivity effects on magnetoHydrodynamic Prandtl nanofluid in a divergent–convergent channel: Drug system applications, Proc IMechE Part E: J Process Mechanical Engineering, 2022: 0749.

4- M. G. Ibrahim, Adaptive simulations to pressure distribution for creeping motion of Carreau nanofluid with variable fluid density effects: Physiological applications, Thermal Science and Engineering Progress, 32 (1) 2022, 101337.

5- W. M. Hasona, A.A. El-Shekhipy, M.G. Ibrahim, Combined effects of magnetohydrodynamic and temperature-dependent viscosity on peristaltic flow of Jeffrey nanofluid through a porous medium: Applications to oil refinement, International Journal of Heat and Mass Transfer, 126 (2018) 700–714.

6- M. G. Ibrahim, Numerical simulation for non-constant parameters effects on blood flow of Carreau–Yasuda nanofluid flooded in gyrotactic microorganisms: DTM-Pade application, Archive of Applied Mechanics, 92 (2022) 1643–1654.

7- M. G. Ibrahim, Concentration-dependent viscosity effect on magnet nano peristaltic flow of Powell-Eyring fluid in a divergent-convergent channel, International Communications in Heat and Mass Transfer, 134, 2022, 105987.

8- N. T. Eldabe, G. M. Moatimid, M. Y. Abouzeid, A. A. ElShekhipy and N. F. Abdallah, A semianalytical technique for MHD peristalsis of pseudoplastic nanofluid with temperature- dependent viscosity: Application in drug delivery system, Heat Transfer-Asian Research 49 (2020), 424– 440.

9- M. G. Ibrahim, Numerical simulation to the activation energy study on blood flow of seminal nanofluid with mixed convection effects, Computer Methods in Biomechanics and Biomedical Engineering, 2022, 2063018.

10- M. G. Ibrahim, Naglaa Abdallah, and Mohamed Abouzeid, Activation energy and chemical reaction effects on MHD Bingham nanofluid flow through a non-Darcy porous media, Egyptian Journal of Chemistry, 2022.117814.5310.

11- M. Y. Abou-zeid, Implicit homotopy perturbation method for MHD non-Newtonian nanofluid flow with Cattaneo-Christov heat flux due to parallel rotating disks, Journal of nanofluids 8(8) (2019), 1648-1653.

12- M. G. Ibrahim and Hanaa A. Asfour, The effect of computational processing of temperature- and concentration-dependent parameters on non-Newtonian fluid MHD: Applications of numerical methods, Heat Transfer, 55, 2022, 1-18.

13- N. T. M. Eldabe, M. Y. Abou-zeid, M. E. Ouaf, D. R. Mustafa and Y. M. Mohammed, Cattaneo – Christov heat flux effect on MHD peristaltic transport of Bingham nanofluid through a non – Darcy porous medium Int. J. Appl. Electromag. Mech. 68 (2022), 59-84.

14- M. G. Ibrahim, W. M. Hasina and A. A. ElShekhipy, Instantaneous influences of thermal radiation and magnetic field on peristaltic transport of Jeffrey nanofluids in a tapered asymmetric channel: Radiotherapy of oncology treatment, Advances, and Applications in Fluid Mechanics, 24(1-2) (2021) 25-55.

15- M. G. Ibrahim, W.M. Hasona and A.A. ElShekhipy, Concentration-dependent viscosity and thermal radiation effects on MHD peristaltic motion of Synovial Nanofluid: Applications to rheumatoid arthritis treatment, Computer Methods and Programs in Biomedicine 170 (2019) 39–52.

16- W. Hasona, Nawal H. Almalki, Abdelhafeez A. El-Shekhipy and M. G. Ibrahim, Combined Effects of Variable Thermal Conductivity and Electrical Conductivity on Peristaltic Flow of Pseudoplastic Nanofluid in an Inclined Non-Uniform Asymmetric Channel: Applications to Solar Collectors, Journal of Thermal Science and Engineering Applications, (2020) 12(2): 021018.

17- W. M. Hasona, A. El-Shekhipy and M. G. Ibrahim, Semi-analytical solution to MHD peristaltic flow of a Jeffrey fluid in presence of Joule heat effect by using Multi-step differential transform method, New Trends In Mathematical Science, 7 (2019) 123-137.

18- N. T. Eldabe, R. R. Rizkallah, M. Y. Abou-zeid & V. M. Ayad, Effect of induced magnetic field on non-Newtonian nanofluid Al2O3 motion through boundary-layer with gyrotactic, Thermal Science, vol. 26, no. 1B, pp. 411-422, 2022.

19- W. M. Hasona, N. H. Almalki, A. A. ElShekhipy, M. G. Ibrahim, Thermal radiation and variable electrical conductivity effects on MHD peristaltic motion of Carreau nanofluids: Radiotherapy and thermotherapy of oncology treatment, Heat Transfer—Asian Res., 55 (2019) 1-19.

20- W. Hasona, N. Al-Malki, A. A. El-Shekhipy, and M. G. Ibrahim, Combined Effects of Thermal Radiation and Magnetohydro-dynamic on Peristaltic Flow of Nanofluids: Applications to Radiotherapy and Thermotherapy of Cancer, Current NanoScience, 16(1), (2020) 121-134.

21- T. Salahuddin, A. M. Bashir, M. Khan and Y. Elmasry, Activation energy study for peristaltically driven divergent flow with radiation effect, Case Studies in Thermal Engineering, 27, (2021) 101172.

22- Z. Shafique, M. Mustafa and A. Mushtaq, Boundary layer flow of Maxwell fluid in rotating frame with binary chemical reaction and activation energy, Results in Physics, 6 (2016) 627-633.

23- R. J. P. Gowda, R. N. Kumar, A. M. Jyothi, B. C. kumara and L. E. Sarris, Impact of binary chemical reaction and activation energy on heat and mass transfer of marangoni driven boundary layer flow of a non-Newtonian nanofluid, Processes, 2021, 9, 702.

24- D. Borah and M.K. Baruah, Proposed novel dynamic equations for direct determination of activation energy in non-isothermal isothermal systems, Fuel processing technology, 86(2005) 781-794.

25- Wang, Jenqdaw; Raj, Rishi, Estimate of the Activation Energies for Boundary Diffusion from Rate-Controlled Sintering of Pure Alumina, and Alumina Doped with Zirconia or Titania. Journal of the American Ceramic Society. 73 (5), (1990), 1172.

26- A. Kiraci, H. Yurtseven, Temperature Dependence of the Raman Frequency, Damping Constant and the Activation Energy of a Soft-Optic Mode in Ferroelectric Barium Titanate. Ferroelectrics. 432 (2012) 14–21.

27- S. Anuradha and M. Yegammai, MHD radiative boundary layer flow of nanofluid past a vertical plate with effects of binary chemical reaction and activation energy, Global Journal of Pure and Applied Mathematics, 13, 9 (2017) 6377-6392.

28- M. G. Ibrahim, N. A. Fawzy, Arrhenius energy effect on the rotating flow of Casson nanofluid with convective conditions and velocity slip effects: Semi-numerical calculations, Heat Transfer, 55, 2022.

29- M. Karabi and A. J. Moghadam, Non-Newtonian Fluid Flow and Heat Transfer in a Semicircular Microtube Induced by Electroosmosis and Pressure Gradient" J. Heat Transfer- Transactions of the ASME, 140(12): 122403, (2018).

30- M. G. Ibrahim and Mohamed Abouzeid, Influence of variable velocity slip condition and activation energy on MHD peristaltic flow of Prandtl nanofluid through a non-uniform channel, Scientific Reports 12(1), 2022.

31- Y.Y. Liang, G.A.F. Weihs, D.F. Fletcher, CFD study of the effect of unsteady slip velocity waveform on shear stress in membrane systems, Chem. Eng. Sci. 192 (2018) 16–24.

32- Z. Nisar, T. Hayat, A. Alsaedi, B. Ahmad, Significance of activation energy in radiative peristaltic transport of Eyring Powell nanofluid, Int. Commun. Heat Mass Transf. 116 (2020) 104655.

33- N. S. Akbar and S. Nadeem, Thermal and velocity slip effects on the peristaltic flow of a six constant Jeffrey's fluid model, International Journal of Heat and Mass Transfer, 55 (2012) 3964-3970.

34- N. T. Eldabe, M. Y. Abou-zeid, M. A. Mohamed and M. Maged, Peristaltic flow of Herschel Bulkley nanofluid through a non-Darcy porous medium with heat transfer under slip condition, Int. J. Appl. Electromag. Mech. **66** (2021), 649-668.

35- A. J. Abuiyada, N. T. Eldabe, M. Y. Abou-zeid & S. M. El Shaboury, Effects of thermal diffusion and diffusion thermo on a chemically reacting MHD peristaltic transport of Bingham plastic nanofluid, Journal of Advanced Research in Fluid Mechanics and Thermal Sciences, vol. 98, no. 2, pp. 24–43, 2022.

36- N. T. M. Eldabe, G. M. Moatimid, M. Abou-zeid, A. A. Elshekhipy and N. F. Abdallah, Semi-analytical treatment of Hall current effect on peristaltic flow of Jeffery nanofluid, Int. J. Appl. Electromag. Mech., 7 (2021), 47-66.

37- Eldabe, N. T., Abouzeid, M. Y. Mohamed, M. A. A., Abd-Elmoneim, M. M. Peristaltic mixed convection slip flow of a Bingham nanofluid through a non-darcy porous medium in an inclined non-uniform duct with viscous dissipation and radiation. J. Appl. Nonlinear Dyn. 12, 231-243 (2023).

38- N. T. Eldabe, M. Y. Abou-zeid, A, Abosaliem, A. Alana & N. Hegazy, Homotopy perturbation approach for Ohmic dissipation and mixed convection effects on non-Newtonian nanofluid flow between two co-axial tubes with peristalsis, International Journal of Applied Electromagnetics and Mechanics, vol. 67, no. 2, pp. 153–163, 2021.

39- A.M. Ismael, N.T.M. Eldabe, M.Y. Abou-zeid and S.M Elshabouri, Thermal micropolar and couple stresses effects on peristaltic flow of biviscosity nanofluid through a porous medium. Scientific Reports 12 (2022), 16180.
40- Abuiyada, A. Eldabe, N. T., Abouzeid, M. Y. Elshabouri, S. Influence of both Ohmic dissipation and activation energy on peristaltic transport of Jeffery nanofluid through a porous media, CFD Letters 15, Issue 6 (2023) 65-85.
41- Abdelmoneim, M., Eldabe, N.T., Abouzeid, M.Y., Ouaf, M.E.: Both modified Darcy's law and couple stresses effects on electro-osmotic flow of non-Newtonian nanofluid with peristalsis. Int. J. Appl. Electromagn. Mech. 72(3), 253–277 (2023).
42- Shaaban, A.A., Abou-Zeid, M.Y. Effects of heat and mass transfer on MHD peristaltic flow of a non-newtonian fluid through a porous medium between two co-axial cylinders, Mathematical Problems in Engineering, 819683 (2013).
43- HA. Sayed and M.Y. Abouzeid, Radially varying viscosity and entropy generation effect on the Newtonian nanofluid flow between two co-axial tubes with peristalsis. Scientific Reports 13 (2023), 11013.
44- M.Y. Abouzeid, Chemical reaction and non-Darcian effects on MHD generalized Newtonian nanofluid motion, Egyptian Journal of Chemistry, 65(12) (2022), 647-655.
45- Abou-Zeid, M.Y., Shaaban, A.A., Alnour, M.Y.: Numerical treatment and global error estimation of natural convective effects on gliding motion of bacteria on a power-law nanoslime through a non-Darcy porous medium. J. Porous Media. 18, (2015)
46- Eldabe, N. T., Abou-zeid M.Y. & Younis, Y. M., Magnetohydrodynamic peristaltic flow of Jeffry nanofluid with heat transfer through a porous medium in a vertical tube. Appl. Math. Inf. Sci. 11(4), 1097–1103 (2017).
47- Eldabe, N. T., Abouzeid, M. Y. & Ahmed, O. S. Motion of a thin film of a fourth grade nanofluid with heat transfer down a vertical cylinder: Homotopy perturbation method application. J. Adv. Res. Fluid Mech. Therm. Sci., 66(2), 101-113 (2020).
48- Mohamed, Y. M., Eldabe, N. T., Abou-zeid, M. Y., Mostapha, D. R. & ouaf, M. E., Impacts of chemical reaction and electric field with Cattaneo - Christov theories on peristaltic transport of a hyperbolic micropolar nanofluid, Egyptian Journal of Chemistry, 66 (7) (2023) 63 – 85.
49- N. T. Eldabe, S. M. El Shaboury, H. A. El Arabawy, Hassan, M. Y. Abou-zeid, & A. Abuiyada, Wall properties and Joule heating effects on MHD peristaltic transport of Bingham non-Newtonian nanofluid, International Journal of Applied Electromagnetics and Mechanics, vol. 69, no. 1, pp. 87-106, 2022.
50- N. T. Eldabe, M. Y. Abou-zeid , A. S. Abo Seliem, A. A. Elenna, & N. Hegazy, Thermal diffusion and diffusion thermo effects on magnetohydrodynamics transport of non-Newtonian nanofluid through a porous media between two wavy co-axial tubes, IEEE Transactions on Plasma Science, vol. 50, no. 5, pp. 1282 - 1290, 2021.
51- Ismael, N. T. M. Eldabe, M. Abouzeid, S. Elshabouri, Entropy generation and nanoparticles Cu O effects on MHD peristaltic transport of micropolar non-Newtonian fluid with velocity and temperature slip conditions, Egyptian Journal of Chemistry, 65 (2022) 715-722.
52- M. E. Ouaf, M. Abouzeid, and Y. M. Younis, Entropy generation and chemical reaction effects on MHD non-Newtonian nanofluid flow in a sinusoidal channel, International Journal of Applied Electromagnetics and Mechanics 69(1) (2022) 1-21.
53- N. T. M. Eldabe, M. Abouzeid, H. A. Shawky, MHD Peristaltic Transport of Bingham Blood Fluid with Heat and Mass Transfer Through a Non-Uniform Channel. Journal of Advanced Research in Fluid Mechanics and Thermal Sciences, 77(2) (2020) 145–159.
54- H. M. Mansour and M. Y. Abou-zeid, Heat and mass transfer effect on non-Newtonian fluid flow in a non-uniform vertical tube with peristalsis, Journal of Advanced Research in Fluid Mechanics and Thermal Sciences, 61(1)(2019), 44-62,
55- Eldabe, N. T., and Abouzeid, M. Y. & Ali, H. A., Effect of heat and mass transfer on Casson fluid flow between two co-axial tubes with peristalsis, J. Adv. Res. Fluid Mech. Therm. Sci. 76, 54–75 (2020).
56- Eldabe, N.T., Abou-Zeid, M.Y. The wall properties effect on peristaltic transport of micropolar non-newtonian fluid with heat and mass transfer, Mathematical Problems in Engineering, 808062 (2010).
57- Mohamed, Y. M., Eldabe, N. T., Abou-zeid, M. Y., Ouaf, M. E. & Mostapha, D. R., Chemical reaction and thermal radiation via Cattaneo-Christov double diffusion (ccdd) effects on squeezing non-Netonian nanofluid flow between two - parallel plates, Egyptian Journal of Chemistry, 66 (3) (2023) 209 – 231.
58- N. T. Eldabe, M. Y. Abou-Zeid, O. H. El-Kalaawy, S. M. Moawad & O. S. Ahmed, Electromagnetic steady motion of Casson fluid with heat and mass transfer through porous medium past a shrinking surface, Thermal Science, vol. 25, no. 1A, pp. 257-265, 2021.
59- N.T.M Eldabe, M.Y. Abou-zeid, S.M. Elshabouri, T.N. Salama, A.M. Ismael, Ohmic and viscous dissipation effects on micropolar non-Newtonian nanofluid Al2O3 flow through a non-Darcy porous media, Int. J. Appl. Electromagn., 68 209–221 (2022).
60- N. T. M. Eldabe, G. M. Moatimid, M. Abou-zeid, A. A. Elshekhipy and N. F. Abdallah, Instantaneous thermal-diffusion and diffusion-thermo effects on Carreau nanofluid flow over a stretching porous sheet, Journal of Advanced Research in Fluid Mechanics and Thermal Sciences 72 (2020) 142-157.
61- Ouaf, M. E. & Abou-zeid, M., Electromagnetic and non-Darcian effects on a micropolar non-Newtonian fluid boundary-layer flow with heat and mass transfer. Int. J. Appl. Electromagn. Mech. 66, 693-703 (2021).
62- Ouaf, M., Abouzeid, M., Ibrahim, M.G.: Effects of both variable electrical conductivity and microstructural/multiple slips on MHD flow of micropolar nanofluid. Egypt. J. Chem. 66, 449–456 (2023).
63- O. S. Ahmed, N. T. Eldabe, M. Y. Abou-zeid, O. H. El-kalaawy and S. M. Moawad, Numerical treatment and global error estimation for thermal electro-osmosis effect on non-Newtonian nanofluid flow with time periodic variations, Sci. Rep. 13 (2023) 14788.

64- MG. brahim and M.Y. Abouzeid, Computational simulation for MHD peristaltic transport of Jeffrey fluid with density-dependent parameters. Scientific Reports 13 (2023), 9191.

65- Mostafa, Y., El-Dabe, N., Abou-Zeid, M., Oauf, M., Mostapha, D.: Peristaltic Transport of Carreau Coupled Stress Nanofluid with Cattaneo-Christov Heat Flux Model Inside a Symmetric Channel. J. Adv. Res. Fluid Mech. Therm. Sci. 98(1), 1-17 (2022)

66- Hegazy, N., Eldabe, N.T., Abouzeid, M., Abousaleem, A., Alana, A.: Influence of both chemical reaction and electro-osmosis on MHD non-Newtonian fluid flow with gold nanoparticles. Egypt. J. Chem. 66, 191 - 201 (2023)